Asian J. Energy Environ., Vol. 5, Issue 4, (2004), pp. 309-325

Temperature Dependence and Photoconductivity Characteristics of Pulsed Laser Deposited Amorphous Carbon Nitride Films for Solar Cell Applications

M. Rusop[1], S. M. Mominuzzaman[2],
T. Soga[1], T. Jimbo[1] and M. Umeno[3]

[1] Department of Environmental Technology and Urban Planning, Nagoya Institute of Technology,
Nagoya 466-8555, Showa-ku, Gokiso-cho, Japan

[2] Department of Electrical and Electronic Engineering,
Bangladesh University of Engineering & Technology, Dhaka 1000, Bangladesh

[3] Department of Electronic Engineering,
Chubu University, Kasugai 487-8501,
Matsumoto-cho 1200, Japan

Email: rusop@mail.com

(Received : 31 January 2004 – Accepted : 15 March 2004)

Abstract : Amorphous carbon nitride films (a-C:N) are deposited by pulsed laser deposition technique at room temperature using a camphoric carbon target with different nitrogen partial pressures in the range from 0.1 to 800 mTorr. The room temperature

conductivity ($\Omega_{RT)}$ found to increase with N incorporation may be due to the lattice vibrations leading to the scattering of the charge carriers by the N atoms and the more amorphous nature of carbon films. Study of activation energy reveals that the Fermi level of the n-C film moves from the valence band to near the conduction band edge through the midgap. The current-voltage photovoltaic characteristics of n-C/p-Si cells under 1 sun air-mass 1.5 (AM 1.5) illumination condition (100 mW/cm^2, 25^{o}C) are improved up to 30 mTorr and deteriorate thereupon. The maximum open circuit voltage $_{(Voc)}$ and short circuit current density $_{(Jsc)}$ for the cells are observed to be approximately 292 mV and 9.02 mA/cm^2, respectively. The highest energy conversion efficiency (~) and fill factor (FF) were found to be approximately 1.47% and 56%, respectively.

Keywords: Photovoltaic; Nitrogen doping; Amorphous carbon nitride; Pulsed laser deposition.

Introduction

Amorphous carbon (a-C) shows semiconducting nature, which promotes its application in the field of semiconductor technology, such as fabrication of photovoltaic solar cells [1]. However, undoped a-C is a weak p-type [1] in nature and the complex structure and presence of high density of defects restricts its ability to dope efficiently and is the main barrier for its application in various electronic devices and therefore, when we attempt to utilize such carbon as alternative material in

optoelectronic devices, control of the conduction type through doping of carbon film is indispensable. The doping mechanism of amorphous semiconductors has always been an interesting issue. Observations from the literature show that the semiconducting carbon films can be either intrinsic or they can be doped during or after the growth to make them extrinsic semiconductors. Effective doping can modify electronic properties, especially gap states, conductivity, etc. in semiconductor materials. Many attempts have been made to dope carbon films using various elements.

It has been reported that phosphorus (P) is the widely used n-type impurity in silicon [2] and is a possible alternative to N in carbon [2]. Though, since N has smaller radius compared to P and is close to that of carbon, the former would be preferred. Further, the N being gas phase has the advantage of better control of dopant concentration over P in physical deposition systems. Veerasamy et al. reported n-type doping of highly tetrahedral carbon (taC) using solid P [1] and n-type doping in a-C using N gas [3-5]. Also, other authors [6,7] reported N is the common dopant in carbon films with few exceptions. The ability to dope [8] using N gas and P has shown a new direction for the application of the carbonaceous material in electronic devices. However, P and N doping of carbon in order to convert undoped p-type conductivity carbon to n-type [9], in relatively smaller gap of DLC film with an optical gap close to that of single crystal silicon (1.1 eV), which has scope in optoelectronic device applications by PLD technique is not reported, so far.

In this paper, the doping modification of temperature dependence and photovoltaic properties that occur in a-CN_x films when they are deposited at different NP have been investigated and discussed. The objective of this study is to dope slightly p-type a-C to electrically semiconducting n-type a-C for their possible application as semiconductors and optoelectronic devices.

Experimental

The a-CN_x films were deposited on single crystal silicon (Si) (100) and fused quartz (quartz) substrates by PLD using camphoric carbon (CC) target [9] at room temperature with different nitrogen partial pressures in the range from 0.1 to 800 mTorr. The influence of NP in range from 0.1 to 800 mTorr using CC target on the N-doping modification of a-C films have been investigated. The target for each deposition method was ablated by 175 mJ/pulse average laser pulse energy with average laser fluence of 3.4 J/cm^2, laser shots of 900 shots and laser repetition rates of 2 Hz. The substrate was mounted at a distance of 45 mm. The substrate temperature was fixed at 20^{o}C. In order to ensure a uniform ablation rate, the CC target was rotated at each 50 shots. The deposition chamber was evacuated to a base pressure approximately at 2×10^{-6} Torr using a turbomolecular pump, and after that, N gas ambient was allowed until the chamber pressure is allayed at setting NP. For comparison, the undoped a-C film was also deposited using pure CC target, thereafter referred to as Sample A. All the films and

photovoltaic cells were analyzed by using standard experimental characterization techniques [9].

Results and Discussions

X-ray photoelectron spectroscopy (XPS) analysis is one of the most likely used techniques in the literature to characterize the formation, bond types and useful information on the chemical environment. XPS shows the C 1s peak position is increased to 284.9 eV (Sample A: 284.8 eV, graphite: 284.25 eV, and diamond: 285.8 eV) at 0.1 mTorr, may be due to the formation of C-N bond which caused the tetrahedral (sp^3) bond increase [9]. The C 1s and N 1s peaks are almost unchanged up to 1 mTorr.

With further increase of NP, the C 1s and N 1s peaks become narrow, indicating the enhancement degree of crystallization in the films. Further, the C 1s peak shifts toward lower binding energy and approaches the binding energy of graphite to 284.35 eV at 30 mTorr (Fig. 1 and 2). This indicates the bonding state of the films changes from low diamond-like, sp^3 bonding to graphite-like trihedral, sp^2 bonding. Above 30 mTorr, the C 1s peak shifts toward higher binding energy and reached at 284.6 eV at 800 mTorr. This indicates the bonding state of the films changes from graphite-like, sp^2 bonding to diamond-like, sp^3 bonding. The presence of oxygen is probably related to the incorporation of oxygen due to prolonged exposure of the samples to the experimental atmosphere before XPS measurements and accidental incorporation during deposition [9]. As shown in Figure 3, the atomic percentage (at%) of N/C (N content) in the a-

C:N films increased rapidly initially up to about 2.93 at% at 50 mTorr. With further increase of NP, the N content increases to about 3.41 at% at 200 mTorr, and saturates thereupon to reach about 3.49 at% at 800 mTorr.

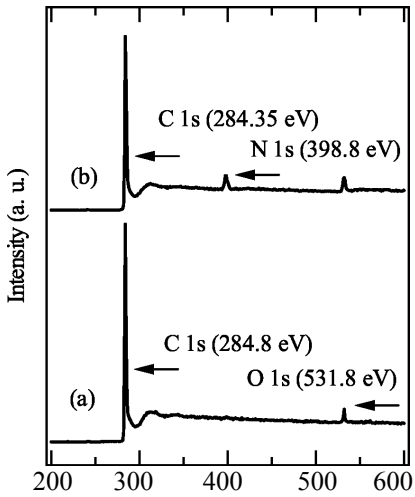

Figure 1. Core level X-ray photoelectron spectra of carbon (C 1s), nitrogen (N 1s) and oxygen (O 1s) for (a) Sample A, and (b) a-C:N film deposited at 30 mTorr.

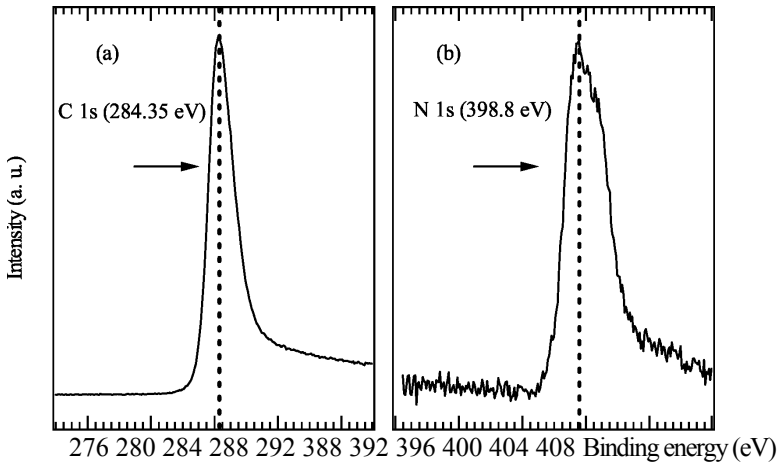

Figure 2. Core level X-ray photoelectron spectra of (a) carbon (C 1s) and (b) nitrogen (N 1s) for a-C:N film deposited at 30 mTorr.

The bonding states of carbon (C), nitrogen (N) and hydrogen (H) atoms can be characterized by Fourier transform infrared spectroscopy (FTIR) measurements. FTIR spectra (Fig. 4) show for a-C:N films, contributions around 1350 and 1550 cm^{-1} were initiated from disordered (D band) and graphite like (G band) CN bonds [10]. Another contribution, around 1212 - 1265 cm^{-1}, was due to symmetric tetrahedral CN bond [11]. At 0.1 mTorr single broad band centered at around 1365 cm^{-1}, almost unchanged up to 1 mTorr, but rapidly shifted later at 10 mTorr into a single broad band centered at around 1550 cm^{-1}. The FTIR absorption remained almost unchanged with higher NP up to 30 mTorr and gradually resolved into two smaller bands located at 1550 and 1200 cm^{-1}. With higher NP, these two bands become more prominent but transformed later at 600 mTorr, into a single broad band centered at around 1200 cm^{-1}, and almost unchanged with higher NP thereafter.

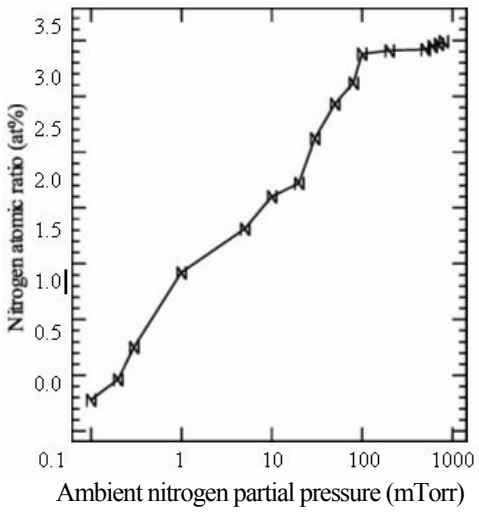

Figure 3. Nitrogen atomic percentage in the a-C:N films as a function of ambient nitrogen partial pressures.

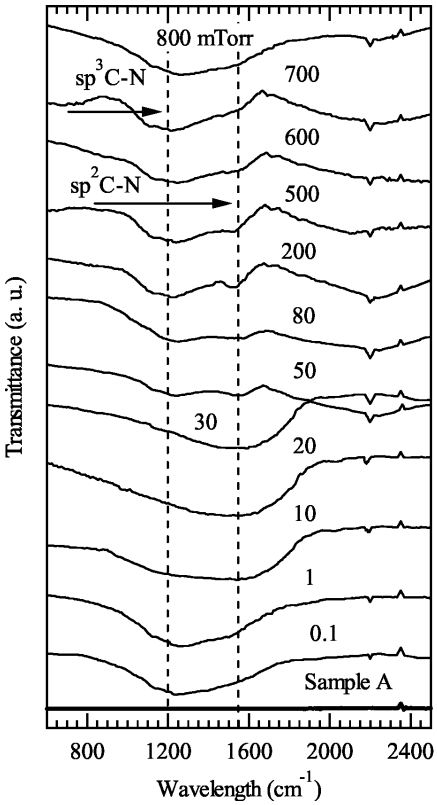

Figure 4. FTIR spectra of Sample A, and a-C:N films with their corresponding ambient nitrogen partial pressures.

Above 30 mTorr, the G band seems to be suppressed gradually, together with the enhancement of the sp^3 CN bonds. This indicates no modification of the binding geometry at low NP up to 1 mTorr and a modification of the binding geometry with the transformation of the sp^3 C-N bonds into sp^2 C-N binding state as NP increased up to 10 mTorr and almost in stable condition with the addition of NP up to 30 mTorr. Whereas, a modification of the binding geometry with the transformation of the sp^2 C-N bonds into sp^3 C-N binding state as NP increased up

to 600 mTorr and almost in stable condition with the addition of NP up to 800 mTorr.

The Tektronix VX1410 IntelliFrame from Sony was used for current-voltage (I-V) measurement and the Cryomini Compressor from Iwatani Plantech was used to maintain the temperature of the chamber (Hereafter, also referred to as 2-probe method). The electron-beam-evaporated gold electrodes (Thickness = 100 nm) were used in a gap cell configuration and silver paste was used as a point contact on gold electrodes for conductivity measurements (Figure 5). From the results of measurements, the electrical conductivity (η) is plotted against inverse temperature (T) on a logarithmic scale. As shown in Figure 6, the temperature dependent conductivity of the films was measured as a function of T between 50 K and 400 K. The T dependence shows two regions, in the 50 to 300 K (variable range hopping) and above 300 K range (simple activation region), which indicate domination of the hopping conductivity of the films. The conductivity plotted in Figure 6 does not follow the simple activated form of (T) = 01exp(-E_a/kT), where $_{01}$ is the conductivity prefactor, T is the absolute temperature, k is Boltzman's constant and E_a is the activation energy with respect to the Fermi level, EF [12]. Since a linear region is not observed for any particular range of temperature, activation energies, E_a are determined from the slope of the straight parts of logarithmic conductivity curves plotted as a function of inverse temperature from the highest temperature side [12] of the two temperature regions (400 K T 300 K and 300 K T 50 K).

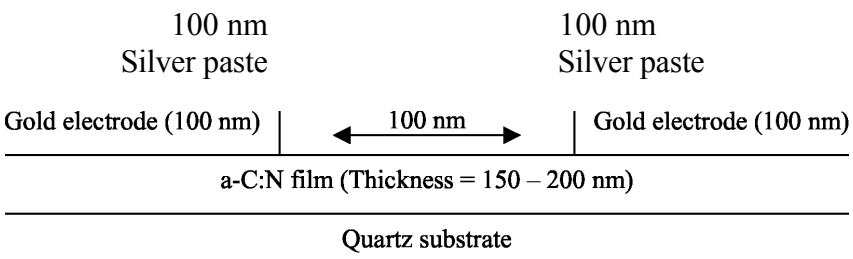

Figure 5. Schematic gap cell configuration for temperature dependent conductivity measurement of a-C:N films deposited in various ambient nitrogen partial pressures.

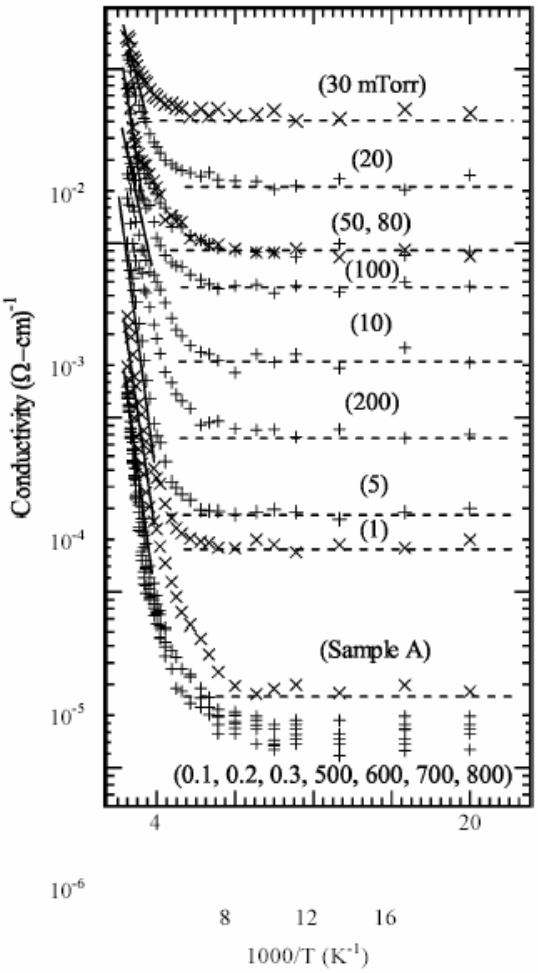

Figure 6. Temperature dependent conductivity of Sample A, and a-C:N films deposited in various ambient nitrogen partial pressures.

Therefore, the activation energy (E_a) is determined from the slope of ln versus 1/T for the above room temperature (RT) region [9,12]. The variation of the E_a and RT conductivity (Ω_{RT}) as a function of NP is shown in Figure 7a (left-axis) and Figure 7a (right axis), respectively. At 0.1 mTorr, the E_a is increased to 0.29 eV (Sample A: 0.24 eV), whereas RT is decreased to 1.3×10^{-5} $(\Omega\text{-cm})^{-1}$ (Sample A: 5.2×10^{-5} $(\Omega\text{-cm})^{-1}$). With a further increase of NP up to 30 mTorr, the E_a decreases, whereas Ω_{RT} increases gradually and sharply thereafter. Above 30 mTorr the E_a and Ω_{RT} are increased with NP.

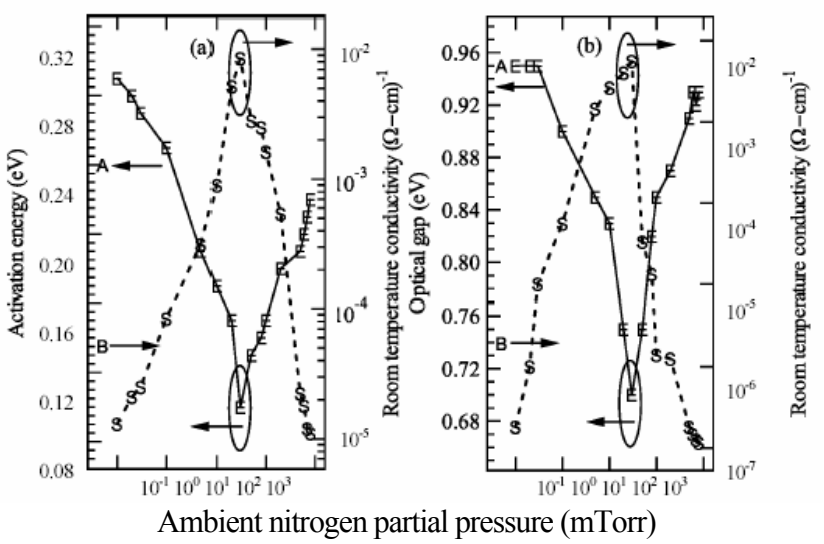

Figure 7. Activation energy (E_a), room temperature conductivity (Ω_{RT}) and optical gap (E_g) of Sample A, and a-C:N films deposited in various ambient nitrogen partial pressures. (a) Left-axis: E_a of Sample A (A) and a-C:N films (E). Right-axis: $_{RT}$ of Sample A (B) and aC:N films measured by 2-probe method (S). (b) Left-axis: E_g of Sample A (A) and a-C:N films (E). Right-axis: $_{RT}$ of Sample A (B) and a-C:N films measured by 4-probe method (S).

For comparison, Ω_{RT} have also been measured by using 4-point probe resistance measurement (Hereafter, also referred to as 4-probe method). The Ω_{RT} measured by 4-probe method (figure 7b (right-axis)) also shows almost the same conductivity characteristics as RT measured by 2-probe method (Figure 7a (left-axis)), with maximum conductivity for the aC:N films deposited at 30 mTorr, which decrease in lower and higher NP.

The electrical conductivity (η) plotted against inverse temperature (T) on a logarithmic scale is shown in Figure 1. The increase in room temperature conductivity (ΩRT) with N incorporation may be due to the lattice vibrations leading to the scattering of the charge carriers by the N atoms and more amorphous nature of the carbon films. However, from 1 to 30 mTorr, the variation of optical band gap (E_g) and electrical properties can be related due to graphitization of a-C:N films. Perhaps the doping of N accompanied by increase of NP up to 30 mTorr, increases crystallinity and substitutional doping of N thereby sharply increases $\Omega_{RT.}$ The increase of E_g and decrease of Ω_{RT} with more N content above 30 mTorr, can be related due to the structural modification in the a-CN_x films as has been confirmed by XPS and FTIR analyses.

The optical properties of the films are investigated by UV-visible spectroscopy measurements in the range of 200 to 2500 nm. Tauc relationship [13] was used to evaluate the optical band gap (E_g). The Tauc optical gap was plotted as a function of NP, as shown in Figure 7b (left-axis). As shown, the E_g of a-C:N films are almost unchanged up to 1 mTorr (Sample A: 0.95 eV),

decreases thereafter to 0.83 eV at 10 mTorr after it decreases rapidly to 0.7 eV at 30 mTorr. With higher NP, it increases to 0.91 eV at 500 mTorr and almost constant thereafter to 0.93 eV at 800 mTorr, as can be estimated from the Tauc plot.

Our results are different to Bhattacharyya et al. [14] where they have observed a gradual decrease of E_g with increase of N content. The decrease in Ω_{RT} with N incorporation, initially at 0.1 Torr may be due to the reason that, as N content increase from null, the incorporated N atoms compensate the dangling bands in the a-C structure and increase the sp^3 fraction. At low NP up to 1 mTorr and upon an increase of NP above 30 mTorr, the variation of E_g and electrical properties can be related to interstitial doping of N in C films through modifications of C-N bonding configurations by rearranging N of atoms.

The increase in Ω_{RT} with N incorporation may also be due to the lattice vibrations leading to the scattering of the charge carriers by the N atoms and more amorphous nature of the carbon films. However, from 1 to 30 mTorr, the variation of E_g and electrical properties can be related due to graphitization of a-C:N films. Perhaps the doping of N accompanied by increase of NP up to 30 mTorr, increases crystallinity and substitutional doping of N thereby sharply increases $\Omega_{RT.}$ The increase of E_g (Fig. 7b) and decrease of Ω_{RT} (Fig. 7a and 7b) with more N content (Fig. 3) above 30 mTorr, can be related due to the structural modification in the a-C:N films as has been confirmed by AFM, SEM and FTIR analyses. Usually this kind of behavior is observed for high content of N in the carbon film, that is for the CN alloy [15,16]. These a-C:N

films might be promising for optical applications as photoconductivity is reported by Nitta et al for CN alloyed film [17].

Photovoltaic solar cells of configurations a-C:P/p-Si have been fabricated. The schematic of the structure of a-C:N films on p-type Si (100) substrates (a-C:N/p-Si) is shown in Figure 8. From the I-V measurement, the I-V characteristics of the n-C:N/p-Si configuration photovoltaic solar cells, without light irradiation, displayed a rectifying I-V characteristic, indicating the formation of heterojunction between the a-C:N films and Si substrates. The cells performance have been given in the dark I-V rectifying curve and I-V working curve under illumination when exposed to AM 1.5 illumination condition (100 mW/cm^2, 25^{o}C). The photovoltaic characteristics are improved with the amount of NP pressures up to 30 mTorr and deteriorate thereupon. The open circuit voltage $_{(Voc)}$ and short circuit current density $_{(Jsc)}$ for cells deposited at 20 mTorr (Fig. 9 (B)) is found to be 273 mV and 8.12 mA/cm^2, respectively. The cell shows efficiency (~) of (1.35%) and fill factor of (FF) (49%).

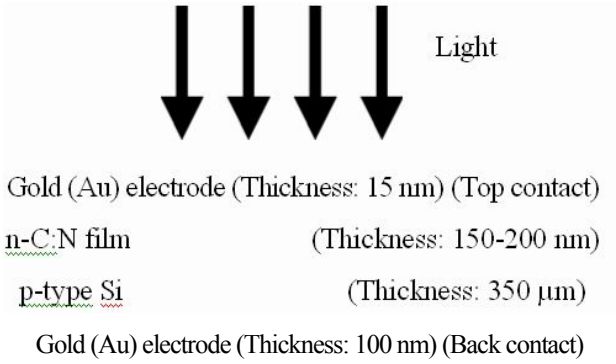

Figure 8. Schematic of the a-C:N/p-Si cell.

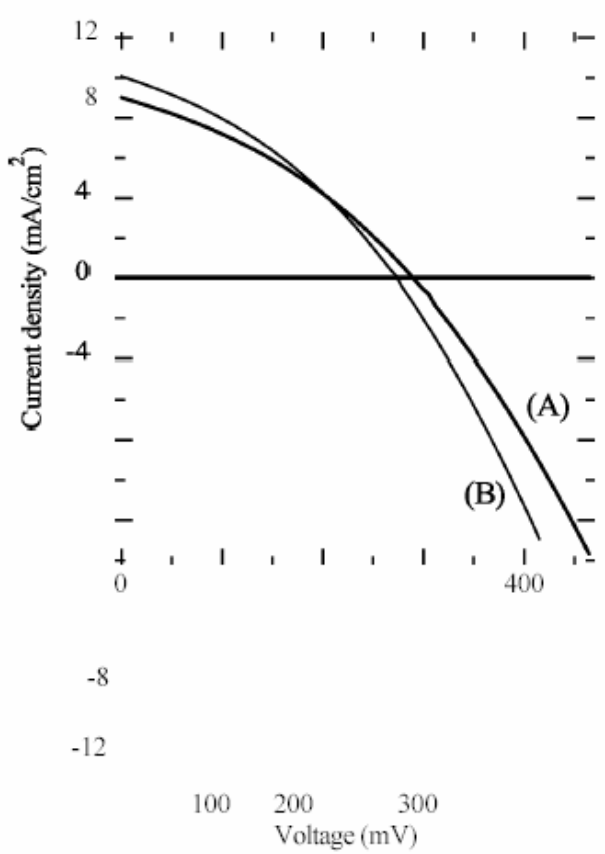

Figure 9. Current-voltage characteristics under illumination of a typical a-C:N/p-Si cells deposited at (A) 30mTorr, and (B) 20 mTorr.

As shown in Figure 9 (A), the maximum of $_{Voc}$ ^{and} $_{Jsc}$ for the cells are observed for the cell deposited at 30 mTorr to be approximately 292 mV and 9.02 mA/cm^2, respectively. This cell shows highest energy conversion efficiency (~) and fill factor (FF) were found to be approximately 1.47% and 56%, respectively.

Conclusions

Amorphous carbon nitride films (a-C:N) are deposited by pulsed laser deposition technique at room temperature using a camphoric carbon target with different nitrogen partial pressures in the range from 0.1 to 800 mTorr. The room temperature conductivity ($\Omega_{RT)}$ found to increase with N incorporation may be due to the lattice vibrations by the N atoms and more amorphous nature of the carbon films. However from 1 to 30 mTorr, the variation of optical band gap (E_g) and electrical properties can be related due to graphitization of a-C:N films. Study of activation energy reveals that the Fermi level of the n-C film moves from the valence band to near the conduction band edge through the midgap. The current-voltage photovoltaic characteristics of n-C/p-Si cells under 1 sun air-mass 1.5 (AM 1.5) illumination condition (100 mW/cm^2, 25^{o}C) are improved up to 30 mTorr and deteriorate thereupon. The maximum open circuit voltage $_{(Voc)}$ and short circuit current density $_{(Jsc)}$ for the cells are observed to be approximately 292 mV and 9.02 mA/cm^2, respectively. The highest energy conversion efficiency (~) and fill factor (FF) were found to be approximately 1.47% and 56%, respectively.

References

[1] Ramasamy, V. S., Amaratunga, G. A. J., Davis, C. A., Timbs, A. E., Milne, W. I. and Mackenzie, D. R. (1993) *J. Phys. Condens. Matter*, **5**, pp.169.

[2] Kadas, K., Ferenczy, G. G. and Kugler, S. (1998) *J. Non-Cryst. Solids*, **227**, pp. 367.

[3] Zhou, Z. B., Cui, R. Q., Pang, Q. J., Hadi, G. M., Ding, Z. M. and Li, W. Y. (2002) *Sol. Energy Mater. and Sol. Cells*, **70**, pp. 487.

[4] Cheah, L. K., Shi, X., Liu, E. and Shi, J. R. (1998) *Appl. Phys. Lett.* **73**, pp. 4273.

[5] Veerasamy, V. S., Yuan, J., Amaratunga, G. A. J., Milne, W. I., Gilkes, K. W. R., Weiler, M. and Brown, L. M. (1993) *Phys. Rev.*, **B 48**, pp. 17954.

[6] Jones, D. I. and Stewart, A. D. (1982) *Philos. Mag.* **B 46**, pp. 423.

[7] M. Alaluf, L. Klibanov and N. Croitoru, Diamond Relat. Mater. **5** (1996) 1497.

[8] Veerasamy, V. S., Yuan, J., Amaratunga, G. A. J., Milne, W. I., Gilkes, K. W. R., Weiler, M. and Brown, L. M. (1993) *Phys. Rev.* **B 48**, pp.17954.

[9] Rusop, M., Mominuzzaman, S. M., Tian, X. M., Soga, T., Jimbo, T. and Umeno, M. (2002) *Applied Surface Science,* **197**, pp. 542.

[10] Hammer, P., Baker, M. A., Lenardi, C. and Gissler, W. (1997) *J. Vac. Sci. Technol*. **A 15**, pp. 107.

[11] Wixom, M. R. (1990) *J. Am. Ceram. Soc.,* **73**, pp.1973.

[12] Orzeszko, S., Bala, W., Fabisiak, K. and Rozploch, F. (1984) *Phys. Status Solidi*, **81**, pp. 579.

[13] Tauc, J., Grigorovici, R. and Vancu, A. (1966) *Phys. Status Solidi,* **15,** pp. 527.

[14] Bhattacharyya, S., Vallee, C., Cardinaud, C., Chauvet, O. and Turban G. (1999) *J. Appl. Phys*. **85**, pp. 2162.